



Universiteit  
Leiden

The Netherlands

## Close the Gap : a study on the regulation of Connexin43 gap junctional communication

Zeijl, L. van

### Citation

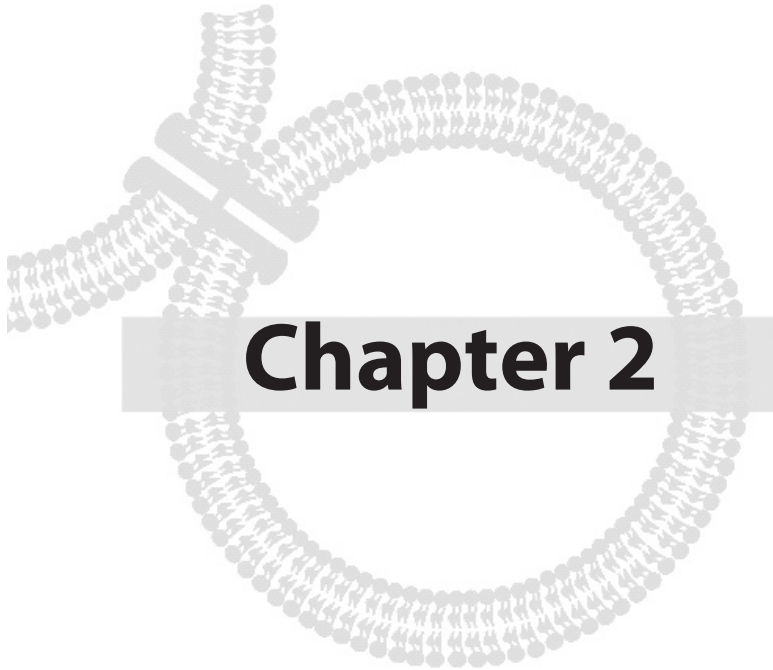
Zeijl, L. van. (2009, May 14). *Close the Gap : a study on the regulation of Connexin43 gap junctional communication*. Retrieved from <https://hdl.handle.net/1887/13799>

Version: Corrected Publisher's Version

License: [Licence agreement concerning inclusion of doctoral thesis in the Institutional Repository of the University of Leiden](#)

Downloaded from: <https://hdl.handle.net/1887/13799>

**Note:** To cite this publication please use the final published version (if applicable).



# Regulation of Connexin43 gap junctional communication by phosphatidylinositol 4,5-bisphosphate

Leonie van Zeijl, Bas Ponsioen, Ben N. G. Giepmans, Aafke Ariaens, Friso R. Postma, Péter Várnai, Tamas Balla, Nullin Divecha, Kees Jalink and Wouter H. Moolenaar

Journal of Cell Biology, 2007 Jun 4;177(5):881-91.



## Abstract

**Cell-cell communication through connexin43 (Cx43)-based gap junction channels is rapidly inhibited upon activation of various G protein-coupled receptors; however, the mechanism is unknown. Here, we show that Cx43-based cell-cell communication is inhibited by depletion of phosphatidylinositol 4,5-bisphosphate (PtdIns(4,5)P<sub>2</sub>) from the plasma membrane. Knockdown of phospholipase Cβ3 (PLCβ3) inhibits PtdIns(4,5)P<sub>2</sub> hydrolysis and keeps Cx43 channels open after receptor activation. Using a translocatable 5-phosphatase, we show that PtdIns(4,5)P<sub>2</sub> depletion is sufficient to close Cx43 channels. When PtdIns(4,5)P<sub>2</sub> is overproduced by PtdIns(4)P 5-kinase, Cx43 channel closure is impaired. We find that the Cx43-binding partner ZO-1 interacts with PLCβ3 via its third PDZ domain. ZO-1 is essential for PtdIns(4,5)P<sub>2</sub>-hydrolyzing receptors to inhibit cell-cell communication, but not for receptor-PLC coupling. Our results show that PtdIns(4,5)P<sub>2</sub> is a key regulator of Cx43 channel function, with no role for other second messengers, and suggest that ZO-1 assembles PLCβ3 and Cx43 into a signalling complex to allow regulation of cell-cell communication by localized changes in PtdIns(4,5)P<sub>2</sub>.**

## Introduction

Communication between adjacent cells through gap junctions occurs in nearly every tissue and is fundamental to coordinated cell behaviour. Gap junctions are composed of connexins, consisting of an intracellular N-terminus, four transmembrane domains and a cytosolic C-terminal tail. Six connexins oligomerize into a pore-forming connexon, and alignment of two connexons in apposing cell membranes forms a gap junction channel. These channels allow direct cell-to-cell diffusion of ions and small molecules (<1-2 kDa), including nutrients, metabolites, second messengers and peptides, without transit through the extracellular space<sup>1-3</sup>. Gap junctions play important roles in normal tissue function and organ development<sup>4-6</sup> and have been implicated in a great diversity of biological processes, notably electrical synchronization of excitable cells, energy metabolism, growth control, wound repair, tumour cell invasion and antigen cross-presentation<sup>7-13</sup>. The importance of gap junctions is highlighted by the discovery that mutations in connexins underlie a variety of genetic diseases, including peripheral neuropathy, skin disorders and deafness<sup>5,14</sup>.

Connexin43 (Cx43) is the most abundant and best studied mammalian connexin. Cx43-based gap junctional communication is of a particular interest since it is regulated by both physiological and pathophysiological stimuli. In particular, Cx43-based cell-cell coupling is rapidly disrupted following stimulation of certain

G protein-coupled receptors (GPCRs), such as those for endothelin, thrombin, nucleotides and bioactive lipids<sup>15-21</sup>. Disruption is transient as communication is restored after about 20-60 min., depending on the GPCR involved<sup>18</sup>. GPCR-mediated inhibition of intercellular communication will have broad consequences for long-range signalling in cells and tissues where Cx43 is vital, such as dermal fibroblasts, glial cells and heart. However, the link between receptor stimulation and Cx43 channel closure has remained elusive to date. Numerous studies on the 'gating' of Cx43 channels have focused on a possible role for phosphorylation of Cx43 by various protein kinases, in particular protein kinase C (PKC), mitogen-activated protein (MAP) kinase and c-Src, but the results remain ambiguous<sup>22-24</sup>. One of the difficulties with unravelling the regulation of Cx43 channel function is that Cx43 functions in a multiprotein complex that is currently ill understood<sup>25</sup>. One established component of this assembly is the scaffold protein ZO-1, which binds directly to the C-terminus of Cx43 via its second PDZ domain<sup>26,27</sup>. ZO-1 has been suggested to participate in the assembly and proper distribution of gap junctions, but its precise role in the Cx43 complex remains unclear<sup>28,29</sup>.

In the present study, we sought to identify the signalling pathway that leads to inhibition of Cx43 gap junctional communication in fibroblasts. Using a variety of experimental approaches, we show that the levels of phosphatidylinositol 4,5-bisphosphate (PtdIns(4,5)P<sub>2</sub>) at the plasma membrane dictate the inhibition (and restoration) of Cx43 gap junctional communication in response to GPCR stimulation, with no role for PtdIns(4,5)P<sub>2</sub>-derived second messengers. We further show that ZO-1, via its third PDZ domain, interacts with phospholipase Cβ3 (PLCβ3) and is essential for Gq/PLC-coupled receptors to abrogate Cx43-based cell-cell communication. Our results suggest a model in which ZO-1 serves to organize Cx43 and PLCβ3 into a complex to allow exquisite regulation of Cx43 channel function by localized changes in PtdIns(4,5)P<sub>2</sub>.

## Results

### *Regulation of Cx43 gap junctional communication by the Gαq-PLCβ-PtdIns(4,5)P<sub>2</sub> hydrolysis pathway*

Rat-1 fibroblasts are ideally suited for studying Cx43 channel function since they express Cx43 as the only functional connexin<sup>18,30</sup>. Stable knockdown of Cx43 expression (using pSuper shRNA) resulted in a complete loss of intercellular communication, consistent with Cx43 being the only functional gap junction protein in Rat-1 cells (Fig. 1A). Fig. 1B shows that the Cx43-binding partner ZO-1 retains its submembranous localization in Cx43 knockdown cells.

To assess which G protein(s) mediate(s) inhibition of gap junctional communication, we introduced active versions of Gαq, Gαi, Gα12 and Gα13 subunits into Rat-1

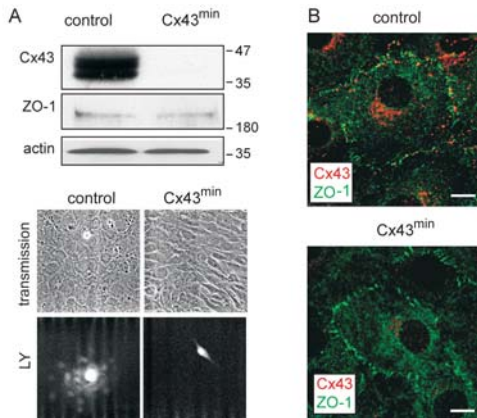


### Figure 1. Cx43 is the only functional connexin in Rat-1 cells

A: Rat-1 cells were transduced with Cx43 shRNA (Cx43<sup>min</sup>) or with a non-functional shRNA (control). Top panel: Immunoblot showing that stable expression of Cx43 shRNA leads to disappearance of Cx43 (Cx43<sup>min</sup> cells), while leaving ZO-1 expression unaltered. Actin served as loading control. Bottom panel: wide-field images of control and Cx43<sup>min</sup> Rat-1 cells. Cx43<sup>min</sup> cells lack cell-cell communication as determined by LY diffusion.

B: Confocal images of control and Cx43<sup>min</sup> cells immunostained for Cx43 (red) and ZO-1 (green) (scale bars, 5  $\mu$ m).

cells and examined their impact on cell-cell coupling. Expression of active G $\alpha$ q resulted in complete inhibition of intercellular communication, whereas active G $\alpha$ i, G $\alpha$ 12 and G $\alpha$ 13 left cell-cell coupling unaltered, as evidenced by Lucifer Yellow (LY) diffusion and electrophysiological assays (Fig. 2A). Disruption of gap junctional communication induced by active G $\alpha$ q was persistent, as opposed to the transient inhibition observed after GPCR stimulation<sup>18</sup>. Similarly, treatment of Rat-1 cells with *Pasteurella multocida* toxin, a direct activator of G $\alpha$ q<sup>31</sup>, caused persistent abrogation of cell-cell coupling (Fig. 2B). G $\alpha$ q couples to PLC $\beta$  to trigger PtdIns(4,5)P<sub>2</sub> hydrolysis leading to production of the second messengers inositol-(1,4,5)-trisphosphate (IP<sub>3</sub>) and diacylglycerol (DAG)<sup>32</sup>. We monitored PtdIns(4,5)P<sub>2</sub> in living cells by using a GFP fusion protein of the PH domain of PLC $\delta$ 1 (GFP-PH) as a probe<sup>33-35</sup>. In control cells, the PtdIns(4,5)P<sub>2</sub> probe was concentrated at the plasma membrane. In cells expressing active G $\alpha$ q, however, the probe was spread diffusely throughout the cytosol, indicative of PtdIns(4,5)P<sub>2</sub> depletion from the plasma membrane (Fig. 2C). While these results are consistent with G $\alpha$ q mediating agonist-induced inhibition of intercellular communication, they should be interpreted with caution since constitutive depletion of PtdIns(4,5)P<sub>2</sub> from the plasma membrane promotes apoptosis<sup>36,37</sup>.

To monitor the kinetics of PtdIns(4,5)P<sub>2</sub> hydrolysis and resynthesis with high temporal resolution, we made use of the fluorescence resonance energy transfer (FRET) between the PH domains of PLC $\beta$ 1 fused to CFP and YFP, respectively<sup>34</sup>. When bound to plasma membrane PtdIns(4,5)P<sub>2</sub>, CFP-PH and YFP-PH are in close proximity and show FRET. Following PtdIns(4,5)P<sub>2</sub> breakdown, the probes dilute out into the cytosol and FRET ceases. The prototypic Gq-coupled receptor agonist endothelin, acting through endogenous ET(A) receptors, induced an acute and substantial decrease in PtdIns(4,5)P<sub>2</sub>, reaching a maximum after 30-60 sec.; thereafter, PtdIns(4,5)P<sub>2</sub> slowly recovered to near basal levels over a period lasting

as long as 45-60 min. (Fig. 2D, upper panel; red trace). Sustained PtdIns(4,5)P<sub>2</sub> hydrolysis by ET(A) receptors has been reported previously<sup>38</sup> and may be explained by the fact that activated ET(A) receptors follow a recycling pathway back to the cell surface rather than the lysosomal degradation route<sup>39</sup>. The kinetics of endothelin-induced inhibition and recovery of cell-cell communication followed those of PtdIns(4,5)P<sub>2</sub> hydrolysis and resynthesis, respectively, with communication being restored after about 75 min. (Fig. 2D, upper panel; black trace).

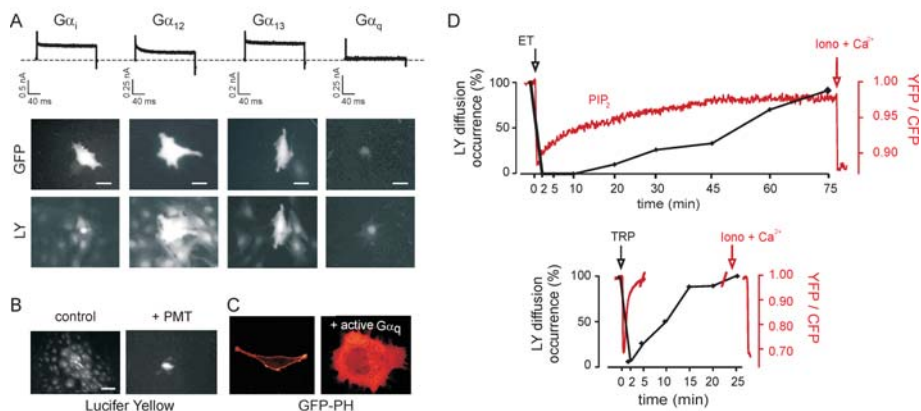


### Figure 2. Activated Gαq disrupts Cx43-based gap junctional communication: correlation with PtdIns(4,5)P<sub>2</sub> depletion.

A: Intercellular communication in Rat-1 cells transfected with various activated (GTPase-deficient) Gα subunits. Upper panel: Electrical cell-cell coupling measured by a single patch-clamp electrode<sup>18</sup>. Whole-cell current responses to 10-mV voltage pulses (duration 100 ms; holding potential -70 mV) were recorded from confluent Rat-1 cells. Note dramatic increase in cellular input resistance (i.e. a decrease in conductance) by activated Gα<sub>q</sub> but not other Gα subunits. Middle and bottom panels: Rat-1 cells cotransfected with active Gα subunits and GFP (10:1 ratio). GFP-positive cells were microinjected with Lucifer Yellow (LY) and dye diffusion from the microinjected cells was monitored. Wide field pictures of GFP and LY diffusion as indicated (scale bars, 10 μm).

B: Disruption of gap junctional communication by *Pasteurella multocida* toxin (PMT; 1 μg/ml; 3 hrs preincubation), an activator of Gα<sub>q</sub>, as measured by LY diffusion (scale bars, 20 μm).

C: Depletion of PtdIns(4,5)P<sub>2</sub> from the plasma membrane by activated Gα<sub>q</sub>. HEK293T cells were transfected with the PtdIns(4,5)P<sub>2</sub> sensor GFP-PH, alone or together with active Gα<sub>q</sub> (1:10 ratio). GFP-PH localizes to the plasma membrane where it binds PtdIns(4,5)P<sub>2</sub> (left panel). Co-expression with activated Gα<sub>q</sub> causes GFP-PH to relocalize to the cytosol (right panel).

D: Monitoring PtdIns(4,5)P<sub>2</sub> levels (PIP<sub>2</sub>; red trace) and intercellular communication (black; n>20 per time point) in Rat-1 cells following addition of endothelin (50 nM) (upper panel) or TRP (50 μM) (lower panel). Data points show the percentage of injected cells that spread LY to their neighbors. Temporal changes in plasma membrane-bound PtdIns(4,5)P<sub>2</sub> were measured by changes in FRET between CFP-PH and YFP-PH. Ionomycin, which evokes an immediate and complete depletion of PtdIns(4,5)P<sub>2</sub> from the plasma membrane when applied at high doses (5 μM) together with 5 mM Ca<sup>2+</sup> (van der Wal *et al.*, 2001) was used for calibration.

More transient PtdIns(4,5)P<sub>2</sub> depletion and recovery kinetics were observed with a thrombin receptor (PAR-1) activating peptide (TRP), which correlated with a more short-lived inhibition of gap junctional communication (Fig. 2D, lower panel). Furthermore, a desensitization-defective mutant NK2 receptor (for neurokinin A) that mediates prolonged PtdIns(4,5)P<sub>2</sub> hydrolysis<sup>40</sup> inhibits gap junctional communication for prolonged periods of time when compared to the wild-type NK2 receptor<sup>18</sup>. While these results reveal a close correlation between the duration of PtdIns(4,5)P<sub>2</sub> depletion and that of communication shutoff, we note that the restoration of cell-cell communication consistently lagged behind the recovery of PtdIns(4,5)P<sub>2</sub> levels. Nevertheless, our findings strongly suggest that the Gq/PLC $\beta$ -mediated hydrolysis and subsequent resynthesis of PtdIns(4,5)P<sub>2</sub> dictate the inhibition and restoration of Cx43 gap junctional communication, respectively.

#### *Knockdown of PLC $\beta$ 3 prevents cell-cell uncoupling*

The G $\alpha$ q-activated PLC $\beta$  enzymes comprise four members ( $\beta$ 1-4)<sup>32</sup>. PLC $\beta$ 1 and  $\beta$ 3 are ubiquitously expressed, whereas PLC $\beta$ 2 and  $\beta$ 4 expression is restricted to hematopoietic cells and neurons, respectively. Rat-1 cells express PLC $\beta$ 3, but no detectable PLC $\beta$ 1 (Fig. 3A and results not shown). We stably suppressed PLC $\beta$ 3 expression using the pSuper short hairpin RNA (shRNA) expression vector<sup>41</sup>. Four different target sequences were selected to correct for clonal variation and off-target effects. Immunoblot analysis shows a marked reduction in PLC $\beta$ 3 expression in different clones (Fig. 3A). When comparing PtdIns(4,5)P<sub>2</sub> dynamics in PLC $\beta$ 3 knockdown versus control cells, agonist-induced PtdIns(4,5)P<sub>2</sub> breakdown was strongly reduced in the PLC $\beta$ 3-deficient cells (Fig. 3B). PLC $\beta$ 3 knockdown cells showed normal basal cell-cell communication but failed to shut off cell-cell communication following GPCR stimulation (Fig. 3C). These results indicate that PLC $\beta$ 3 is a key player in the control of intercellular communication, supporting the view that GPCRs inhibit gap junctional communication through the Gq/PLC $\beta$ -PtdIns(4,5)P<sub>2</sub> hydrolysis pathway.

PLC-mediated PtdIns(4,5)P<sub>2</sub> hydrolysis generates the second messengers IP<sub>3</sub> and DAG, leading to Ca<sup>2+</sup> mobilization and protein kinase C (PKC) activation, respectively. Previous pharmacological studies already suggested that neither Ca<sup>2+</sup> nor PKC have a critical role in GPCR-mediated inhibition of cell-cell coupling<sup>18</sup>, a notion supported by additional experiments using 'caged' IP<sub>3</sub>, the cell-permeable Ca<sup>2+</sup> chelator BAPTA-AM and a PKC-activating bacterial PLC<sup>42</sup> (data summarized in Table S1). Whether PtdIns(4,5)P<sub>2</sub>-derived second messengers are dispensable for Cx43 channel closure upon GPCR activation remains debatable, however, since the supporting pharmacological evidence is indirect.



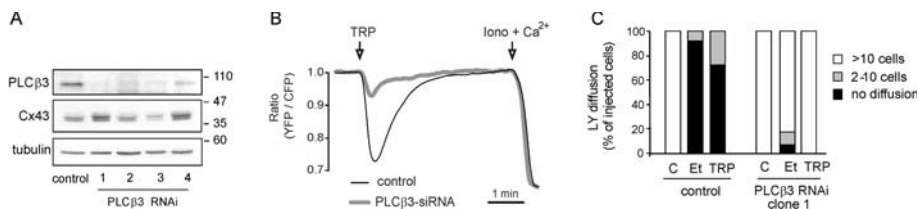


**Figure 3. Targeted knockdown of PLCβ3 prevents receptor-mediated PtdIns(4,5)P<sub>2</sub> hydrolysis and inhibition of junctional communication.**

A: PLCβ3 knockdown in Rat-1 cells as detected by immunoblotting. Expression of PLCβ3 in Rat-1 cells expressing a non-functional shRNA (control) and in four subclones (1-4) stably expressing different PLCβ3 shRNA constructs. Total cell lysates were immunoblotted for PLCβ3, Cx43 and α-tubulin as indicated.

B: Temporal changes in plasma-membrane PtdIns(4,5)P<sub>2</sub> levels following thrombin receptor stimulation of normal (red trace) and PLCβ3-deficient Rat-1 cells (blue trace). TRP, 50 μM; Ionomycin, 5 μM.

C: Bar graphs showing the percentage of communicating cells in control and v PLCβ3 knock-down cells (clone1) treated with either endothelin (Et, 50 nM) or TRP (50 μM), as indicated (n >25 for each dataset). LY injections were done at 2 min. after addition of agonist.

#### *Conversion of PtdIns(4,5)P<sub>2</sub> into PtdIns(4)P by phosphoinositide 5-phosphatase is sufficient to inhibit cell-cell communication*

To examine whether the depletion of PtdIns(4,5)P<sub>2</sub> suffices to inhibit Cx43 gap junctional communication, we used a newly developed method to rapidly deplete PtdIns(4,5)P<sub>2</sub> without activating PLC. In this approach, PtdIns(4,5)P<sub>2</sub> at the plasma membrane is converted into PtdIns(4)P and free phosphate by rapamycin-inducible membrane targeting of the human type IV phosphoinositide 5-phosphatase (5-ptase)<sup>43,44</sup>. The method is based on the rapamycin-induced heterodimerization of FRB (fragment of mammalian target of rapamycin [mTOR] that binds FKBP12) and FKBP12 (FK506-binding protein 12), as schematically illustrated in Fig. 4A. In this approach, a mutant version of 5-ptase with a defective membrane targeting domain (CAAX box) is fused to FKBP12 and tagged with monomeric red fluorescent protein (mRFP), while its binding partner FRB (fused to CFP) is tethered to the plasma membrane through palmitoylation (construct PM-FRB-CFP)<sup>43</sup>. In the absence of rapamycin, 5-ptase resides in the cytosol and leaves PtdIns(4,5)P<sub>2</sub> levels at the plasma membrane unaltered (Fig. 4A, left panel). Upon addition of rapamycin (100 nM), FKBP and FRB undergo heterodimerization and the 5-ptase is recruited to the plasma membrane (Fig. 4A, right panel).

We expressed the mRFP-FKBP-5-ptase and PM-FRB-CFP fusion proteins in Rat-1 cells and confirmed their proper intracellular localization by confocal microscopy (not shown). Addition of rapamycin caused a rapid and complete depletion of PtdIns(4,5)P<sub>2</sub>, as shown by the disappearance of the PtdIns(4,5)P<sub>2</sub> sensor YFP-PH from the plasma membrane (Fig. 4B and 4C, upper trace n=10). As expected, no Ca<sup>2+</sup> signal was detected following the 5-ptase-mediated conversion of PtdIns(4,5)P<sub>2</sub>

into PtdIns(4)P (n=4; Fig. 4C). To determine how the 5-ptase-induced hydrolysis of PtdIns(4,5)P<sub>2</sub> affects gap junctional communication, we measured the intercellular diffusion of calcein (added as membrane-permeable calcein-AM) using FRAP (Fluorescence Recovery After Photobleaching)<sup>45</sup> (Fig. 4D). Rat-1 cells expressing mRFP-FKBP-5-ptase and PM-FRB-CFP showed efficient intercellular transfer of calcein. At 2 minutes after rapamycin addition, however, intercellular dye diffusion was inhibited as inferred from a strongly reduced fluorescence recovery rate (Fig. 4D; n=15, p<0.005; about 0.25 x the recovery rate before rapamycin addition). The recovery of calcein fluorescence could not be decreased any further by addition of the gap junction blocker 2-APB (2-aminoethoxy-diphenylborane; 50 μM; Fig. 4D)<sup>46</sup>.

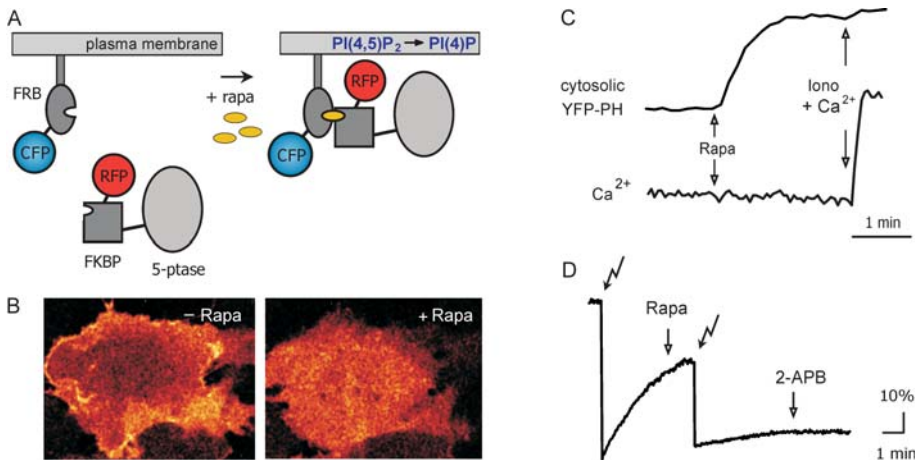


**Figure 4. PtdIns(4,5)P<sub>2</sub> depletion by 5-phosphatase inhibits gap junctional communication.**

A: Schematic representation of rapamycin-induced PtdIns(4,5)P<sub>2</sub> degradation at the plasma membrane. Rapamycin induces dimerization of FKBP domains to FRB domains. Rapamycin recruits the phosphoinositide-5-phosphatase-FKBP fusion protein (mRFP-FKBP-5-ptase) to FRB tethered to the plasma membrane (PM-FRB-CFP), resulting in the rapid conversion of PtdIns(4,5)P<sub>2</sub> into PtdIns(4)P. B: Confocal images of YFP-PH in Rat-1 cells before (left) and after (right) addition of rapamycin (100nM). In addition to YFP-PH, PM-FRB-CFP and mRFP-FKBP-5-ptase were also correctly expressed (images not shown). Note that the translocation of YFP-PH into the cytoplasm is complete, indicative of massive PtdIns(4,5)P<sub>2</sub> hydrolysis. C: Representative responses to rapamycin and ionomycin. Top, cytosolic levels of YFP-PH; bottom, Ca<sup>2+</sup> dye Oregon Green. Ionomycin treatment could not induce further translocation of YFP-PH, indicating that rapamycin-induced PtdIns(4,5)P<sub>2</sub> degradation was complete (n=10). Rises in cytosolic Ca<sup>2+</sup> were never observed (n=4), confirming that PtdIns(4,5)P<sub>2</sub> hydrolysis did not generate second messengers. D; Gap junctional communication in Rat-1 cells transfected with PM-FRB-CFP and mRFP-FKBP-5-ptase, assayed by fluorescence recovery after photobleaching (FRAP) of calcein. While cells showed efficient communication before rapamycin-treatment, gap junctional exchange was significantly decreased at 2 min after addition of rapamycin (0.25 x recovery rate before rapamycin, n=15, p<0.005). The gap junction blocker 2-APB was added at 50 μM.

Rapamycin did not affect cell-cell communication in non-transfected cells (data not shown). Thus, PtdIns(4,5)P<sub>2</sub> depletion by 5-phosphatase activation is sufficient to inhibit Cx43 gap junctional communication, with no need for PtdIns(4,5)P<sub>2</sub>-derived second messengers.

#### *Overexpression of PtdIns(4)P 5-kinase prevents inhibition of cell-cell communication*

PtdIns(4,5)P<sub>2</sub> at the plasma membrane is generated mainly from PtdIns(4)P by PtdIns(4)P 5-kinase (PIP5K)<sup>47,48</sup>. As a further test of the PtdIns(4,5)P<sub>2</sub> hypothesis, we stably overexpressed PIP5K (type I $\alpha$ , fused to GFP) in Rat-1 cells in an attempt to prevent PtdIns(4,5)P<sub>2</sub> depletion following GPCR stimulation (Fig. 5A). As shown in Fig. 5B, transfected GFP-PIP5K localizes to the plasma membrane. In the PIP5K-overexpressing cells, PtdIns(4,5)P<sub>2</sub> levels remain elevated (i.e. above FRET threshold levels) after agonist addition (Fig. 5C). Nonetheless, GPCR agonists still induced transient rises in IP<sub>3</sub> and Ca<sup>2+</sup> (Fig. 5C), indicating that excessive synthesis of PtdIns(4,5)P<sub>2</sub> does not interfere with its hydrolysis. Basal cell-cell communication in PIP5K-overexpressing cells was not significantly different from that in control cells. However, the PIP5K-overexpressing cells failed to close their gap junction channels upon addition of TRP and, to a lesser extent, endothelin (Fig. 5C). That endothelin is still capable of evoking a residual response in PIP5K-overexpressing cells may be explained by the fact that endothelin is by far the strongest inducer of PtdIns(4,5)P<sub>2</sub> depletion (Fig. 2D).

Expression of a 'kinase-dead' version of PIP5K had no effect on either PtdIns(4,5)P<sub>2</sub> hydrolysis or inhibition of cell-cell communication (Fig. 5D). We conclude that Cx43 channel closure is prevented when PtdIns(4,5)P<sub>2</sub> is maintained at adequate levels.

#### *No detectable PtdIns(4,5)P<sub>2</sub> binding to the C-terminal tail of Cx43*

PtdIns(4,5)P<sub>2</sub> can modulate the activity of various ion channels and transporters, apparently through direct electrostatic interactions<sup>49,50</sup>. By analogy, regulation of Cx43 channels by PtdIns(4,5)P<sub>2</sub> would imply that basic residues in Cx43 bind directly to the negatively charged PtdIns(4,5)P<sub>2</sub>. Indeed, the regulatory cytosolic tail of Cx43 (aa 228-382) contains a membrane-proximal stretch of both basic and hydrophobic residues (231VFFKGVKDRVKGK/R243) that could constitute a potential PtdIns(4,5)P<sub>2</sub> binding site. Local depletion of PtdIns(4,5)P<sub>2</sub> might then dissociate the juxtamembrane region of the Cx43 tail from the plasma membrane leading to channel closure. We reasoned that if the Cx43 juxtamembrane domain binds PtdIns(4,5)P<sub>2</sub> *in situ*, mutations within this domain might interfere with PtdIns(4,5)P<sub>2</sub>-regulated channel closure. We therefore neutralized the membrane-proximal Arg and Lys residues by mutation to alanine resulting in eight distinct Cx43 mutants, notably K237A,K241A; R239A,R243A; K241A,R243A; R239A,K241A; K237A,R239A; R239A,K241A,R243A; K237A,R239A,K241A and the '4A' mutant,

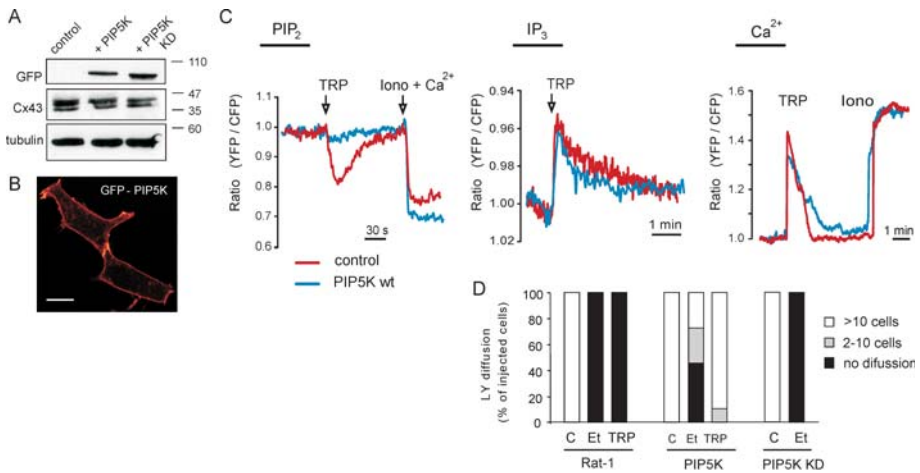


**Figure 5. Overexpression of PtdIns(4)P 5-kinase attenuates agonist-induced PtdIns(4,5)P<sub>2</sub> depletion and keeps junctional communication largely intact.**

(A) Stable expression of GFP-PIP5K (wild-type, WT, and ‘kinase-dead’, KD) in Rat-1 cells. Total cell lysates were immunoblotted for GFP, Cx43 and  $\alpha$ -tubulin as indicated.

(B) Localization of GFP-PIP5K in Rat-1 cells (scale bar, 10  $\mu$ m).

(C) Temporal changes in the levels of PtdIns(4,5)P<sub>2</sub>, IP<sub>3</sub> and Ca<sup>2+</sup> measured by the respective FRET-based sensors, as detailed in the Methods section.

Control and PIP5K-overexpressing Rat-1 cells were stimulated with TRP (50  $\mu$ M). In control cells (red trace), PtdIns(4,5)P<sub>2</sub> levels rapidly fall after TRP stimulation, whereas PIP5K overexpression (blue trace) largely prevents the drop in FRET indicating that PtdIns(4,5)P<sub>2</sub> levels remain high (i.e. above FRET threshold). Ionomycin, 5  $\mu$ M.

(D) Bar graphs showing the percentage of communicating cells (LY diffusion) in control Rat-1 cells and cells expressing either wild-type (wt) or kinase-dead (KD) PIP5 kinase. Cells were left untreated (C) or stimulated with GPCR agonists (endothelin, 50 nM; TRP, 50  $\mu$ M) as indicated (n >20 for each dataset). Residual response to endothelin is explained by excessive depletion of PtdIns(4,5)P<sub>2</sub> (Fig. 2D). LY injections were done at 2 min. after addition of agonist

K237A,R239A,K241A,K243A. When expressed in Cx43-deficient cells, however, all these mutants were trapped intracellularly and failed to localize to the plasma membrane (Fig. S1A). While this result reveals a previously unknown role for the membrane-proximal Arg/Lys residues in Cx43 trafficking, it precludes a test of the Cx43-PtdIns(4,5)P<sub>2</sub> interaction hypothesis.

We next examined whether PtdIns(4,5)P<sub>2</sub> can specifically bind to either the Cx43 C-terminal tail (Cx43CT; aa 228-382) or a Cx43CT-derived juxtamembrane peptide (Cx43JM; aa 228-263) in vitro. We generated a GST-Cx43CT fusion protein and determined its ability to bind phosphoinositides in vitro using three distinct protocols. GST-PH(PLC $\delta$ 1) was used as a positive control. In the first approach, agarose beads coated with either PtdIns(4,5)P<sub>2</sub> or PtdIns(4)P were incubated with GST-Cx43CT or GST-PH and then pulled down by centrifugation. PtdIns(4,5)P<sub>2</sub> beads readily brought down the GST-PH polypeptide but not GST-Cx43CT (Fig. S2A). Second, we incubated GST-Cx43CT with <sup>32</sup>P-labeled PtdIns(4,5)P<sub>2</sub> and examined the ability of excess phosphoinositides to displace bound <sup>32</sup>P-PtdIns(4,5)P<sub>2</sub>.

While GST-PH showed again strong PtdIns(4,5)P<sub>2</sub> binding that could readily be displaced by excess PtdIns(4,5)P<sub>2</sub>, there was no detectable binding of PtdIns(4,5)P<sub>2</sub> to Cx43CT above that observed with GST alone (Fig. S2B). Finally, we found that PtdIns(4,5)P<sub>2</sub> (and other phosphoinositides) immobilized on nitrocellulose strips failed to bind either Cx43CT or a 35-aa juxtamembrane domain peptide (Cx43JM; aa 228-263<sup>55</sup>) (results not shown). Thus, PtdIns(4,5)P<sub>2</sub> does not detectably bind to the juxtamembrane domain of Cx43, nor to the full-length regulatory tail (aa 228-362), at least *in vitro*.

#### *ZO-1 is required for GPCRs to inhibit junctional communication*

The very C-terminus of Cx43 binds directly to the second PDZ domain of ZO-1, but the functional significance of the Cx43-ZO-1 interaction is not understood. We asked if ZO-1 has a role in modulating gap junctional communication in response to GPCR stimulation. We already showed that RNAi-mediated depletion of Cx43 does not significantly affect the levels and localization of ZO-1 (Fig. 1B). Conversely, when ZO-1 expression was knocked down by shRNA, Cx43 levels were unaltered (Fig. 6A). ZO-1 knockdown Rat-1 cells retained their fibroblastic morphology and showed normal Cx43 punctate staining and cell-cell coupling (Fig. 6B,C), showing that ZO-1 is dispensable for the formation of functional gap junctions. When ZO-1 knockdown cells were stimulated with endothelin, however, the inhibition of cell-cell communication was severely impaired (Fig. 6C). Importantly, overall PtdIns(4,5)P<sub>2</sub>-dependent Ca<sup>2+</sup> mobilization was not affected in the ZO-1 knockdown cells (Fig. 6D). We conclude that ZO-1 is essential for the regulation of gap junctional communication by Gq/PLC-coupled receptors, but not for linking those receptors to PLC activation. A plausible explanation for these findings is that ZO-1 serves to bring the PtdIns(4,5)P<sub>2</sub>-metabolizing machinery into proximity of Cx43 gap junctions.

#### *Direct interaction between ZO-1 and PLCβ3*

As a test of the above hypothesis, we examined if ZO-1 can interact with PLCβ3. PLCβ3 can associate with at least two scaffold proteins, NHERF2 (in epithelial cells) and Shank2 (in brain), via a C-terminal PDZ domain-binding motif<sup>51,52</sup>. We co-expressed HA-PLCβ3 and GFP-ZO-1 in HEK293 cells and performed immunoprecipitations using anti-GFP antibody (Fig. 7A). Cell lysates and immunoprecipitates were blotted for GFP and HA. As shown in Fig. 7B, PLCβ3 and ZO-1 can indeed be coprecipitated. Next, we co-expressed ZO-1 and a PLCβ3 truncation mutant that lacks the C-terminal 14 residues (HA-PLCβ3-ΔPBD; Fig. 7A), and performed anti-GFP immunoprecipitations. Fig. 7B shows that truncated PLCβ3 fails to interact with ZO-1, indicating that PLCβ3 interacts with ZO-1 through its very C-terminus, containing the PDZ domain-binding motif. Considering that ZO-1 has three distinct

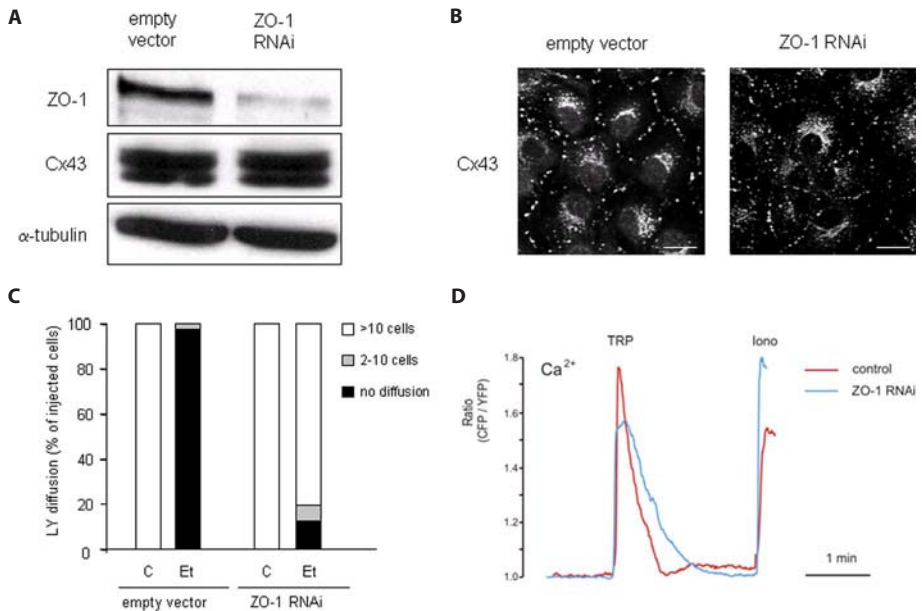


**Figure 6. Knockdown of ZO-1 largely prevents agonist-induced disruption of junctional communication, while leaving Ca<sup>2+</sup> mobilization intact.**

A: Immunoblots showing strongly reduced ZO-1 expression by adenoviral ZO-1 RNAi compared to control virus ('empty vector'). ZO-1 knockdown did not affect Cx43 expression, as indicated.

B: Immunostaining of Cx43 in control and ZO-1 knockdown Rat-1 cells. Note that ZO-1 knockdown does not affect Cx43 punctate staining patterns.

C: Bar graphs showing communication in control ('empty vector') and ZO-1 knockdown cells (ZO-1 RNAi) before and after addition of endothelin (Et, 50 nM) (data sets represent totals of at least two independent experiments; number (n) of injected cells: empty vector -/+ Et, n=53/85; ZO-1 RNAi -/+ Et, n=43/56). LY injections were done at 2 min. after addition of agonist.

D: GPCR-mediated Ca<sup>2+</sup> mobilization in control cells (red trace) and ZO-1 knockdown cells (blue trace). Ca<sup>2+</sup> was measured using the FRET-based Yellow Cameleon probe. TRP, 50  $\mu$ M; Ionomycin, 5  $\mu$ M.

PDZ domains, we examined which (if any) PDZ domain binds PLC $\beta$ 3. We expressed GFP-tagged versions of the three individual PDZ domains in HEK293 cells, either alone or together with HA-PLC $\beta$ 3. We immunoprecipitated PLC $\beta$ 3 using anti-HA antibody and blotted total cell lysates and precipitates for both HA and GFP. As shown in Fig. 7C, we find that PLC $\beta$ 3 binds to PDZ3 but not to PDZ1 or PDZ2.

To verify that the ZO-1-PLC $\beta$ 3 interaction exists endogenously, we precipitated ZO-1 from Rat-1 cells and blotted for both ZO-1 and PLC $\beta$ 3. Fig. 7D shows that PLC $\beta$ 3 co-precipitates with ZO-1. The reverse co-precipitation could not be done, since precipitating antibodies against PLC $\beta$ 3 are presently not available. Nonetheless, these results suggest that ZO-1, through its respective PDZ2 and PDZ3 domains,

assembles Cx43 and PLC $\beta$ 3 into a signalling complex and thereby facilitates regulation of gap junctional communication by PLC-coupled receptors.

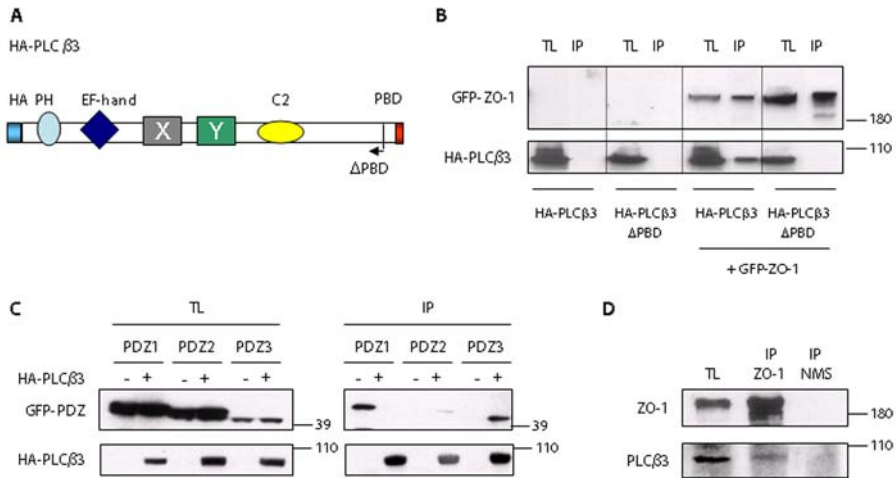


### Figure 7. Association of ZO-1 with PLC $\beta$ 3

A: Schematic representation of HA-PLC $\beta$ 3. X, Y represent the catalytic domains; the C2 domain interacts with activated G $\alpha$ <sup>q</sup>;  $\Delta$ PBD: mutant PLC $\beta$ 3 lacking the C-terminal residues 1220-1234 (comprising the PDZ domain binding motif).

B: Co-immunoprecipitation of GFP-ZO-1 and HA-PLC $\beta$ 3 expressed in HEK293 cells. TL: total cell lysates; IP, denotes immunoprecipitation using anti-GFP antiserum. Samples were immunoblotted for GFP (top) and HA (bottom).

C: Co-immunoprecipitation of HA-PLC $\beta$ 3 and GFP-tagged individual PDZ domains of ZO-1 expressed in HEK293 cells. TL: total cell lysates; IP, denotes immunoprecipitation using anti-HA antibody. Samples were immunoblotted for GFP (top) and HA (bottom).

D: Endogenous ZO-1 immunoprecipitated (IP) from Rat-1 cells. Total cell lysates (TL) and samples from ZO-1 immunoprecipitates (IP) were blotted for both ZO-1 and PLC $\beta$ 3 as indicated. NMS: normal mouse serum.

## Discussion

A critical and long-standing question in gap junction biology is how junctional communication is regulated by physiological and pathophysiological stimuli. Relatively little progress has been made in identifying receptor-induced signalling events that modulate the channel function of Cx43, the best studied and most abundant mammalian connexin. In particular, regulation of Cx43 channel activity via G-protein signalling has not been systematically examined to date. In the present study, we identify the Gq-linked PLC $\beta$ -PtdIns(4,5)P<sub>2</sub> hydrolysis pathway as a key regulator of Cx43-based gap junctional communication in normal fibroblasts. We demonstrate that loss of PtdIns(4,5)P<sub>2</sub> from the plasma membrane is necessary and sufficient to close Cx43 channels, without a role for PtdIns(4,5)P<sub>2</sub>-derived second messengers.

In other words, PtdIns(4,5)P<sub>2</sub> itself is the responsible signalling molecule. A second novel finding is that the Cx43-binding partner ZO-1 binds to PLCβ3 and is essential for PtdIns(4,5)P<sub>2</sub>-hydrolyzing receptors to regulate gap junctional communication.

#### *PtdIns(4,5)P<sub>2</sub> as a key regulator*

Our conclusion that PtdIns(4,5)P<sub>2</sub> at the plasma membrane regulates Cx43 channel function is based on several lines of evidence. First, active Gαq (but not Gαi, Gα12 or Gα13) depletes PtdIns(4,5)P<sub>2</sub> from the plasma membrane and abrogates gap junctional communication. Second, knockdown of PLCβ3 inhibits agonist-induced PtdIns(4,5)P<sub>2</sub> depletion and prevents disruption of cell-cell communication. Third, conversion of PtdIns(4,5)P<sub>2</sub> into PtdIns(4)P by a translocatable 5-phosphatase is sufficient to inhibit intercellular communication. Fourth, maintaining PtdIns(4,5)P<sub>2</sub> at adequate levels by overexpression of PIP5K renders Cx43 channels refractory to GPCR stimulation, although second messenger generation still occurs.

Acting as a signalling molecule in its own right, PtdIns(4,5)P<sub>2</sub> can regulate local cellular activities when its levels rise and fall; in particular, PtdIns(4,5)P<sub>2</sub> can modulate the activity of various ion channels and transporters, presumably through electrostatic interactions<sup>49,50</sup>. Although the existence of such interactions in living cells remains largely inferential and PtdIns(4,5)P<sub>2</sub>-binding consensus sequences have not been clearly defined, the common theme is that the negatively charged PtdIns(4,5)P<sub>2</sub> binds to a motif with multiple positive charges interdispersed with hydrophobic residues<sup>53,54</sup>. The Cx43 C-terminal juxtamembrane domain indeed contains such a putative PtdIns(4,5)P<sub>2</sub>-binding motif (aa 231-243), although this stretch also meets the criteria of α tubulin-binding domain<sup>55</sup>. Extension of the above model to Cx43 channel gating would then imply that local loss of PtdIns(4,5)P<sub>2</sub> could release the Cx43 regulatory tail from the plasma membrane to render it susceptible to a modification leading to channel closure. However, our investigations to detect specific binding of PtdIns(4,5)P<sub>2</sub> to the Cx43 C-terminal tail or its juxtamembrane domain *in vitro* yielded negative results. Rather, mutational analysis revealed that those basic residues in the juxtamembrane domain have a hitherto unrecognized role in the trafficking of Cx43 to the plasma membrane. These findings do not, of course, rule out the possibility that PtdIns(4,5)P<sub>2</sub> does bind directly to Cx43 *in situ*. Aside from modulating ion channel activity, PtdIns(4,5)P<sub>2</sub> has been implicated in cytoskeletal remodeling, vesicular trafficking and recruitment of cytosolic proteins to specific membranes<sup>54,56</sup>. Although Cx43 can interact with cytoskeletal proteins, such as tubulin and drebrin<sup>55,57</sup>, cytoskeletal reorganization does not play a significant role in regulating Cx43 junctional communication because cytoskeleton-disrupting agents (cytochalasin D, nocodazole, Rho-inactivating C3 toxin) have no detectable effect on GPCR regulation of cell-cell coupling<sup>55</sup> (see also Table S1). Furthermore, we found that GPCR-induced inhibition and recovery of gap



junctional communication are insensitive to agents known to interfere with Cx43 trafficking and internalization, including cycloheximide, brefeldin A, monensin, ammonium chloride and hypertonic sucrose (Table S1).

Numerous studies have suggested that closure of Cx43 channels in response to divergent stimuli somehow results from Cx43 phosphorylation<sup>22,23</sup>. Several protein kinases, including PKC, MAP kinase, casein kinase-1 and Src, are capable of phosphorylating Cx43 at multiple sites in the C-terminal tail. These phosphorylations have been implicated not only in Cx43 channel gating but also in Cx43 trafficking, assembly and degradation. The link between Cx43 phosphorylation and altered cell-cell coupling is largely correlative, however, as the functional significance of most of these phosphorylations has not been elucidated. Our previous studies suggested that c-Src-mediated tyrosine phosphorylation of Cx43 underlies disruption of gap junctional communication, as inferred from experiments using both constitutively active and dominant-negative versions of c-Src<sup>18,58</sup>. To date, however, we have been unable to detect GPCR-induced tyrosine phosphorylation of Cx43 in a physiological context. Furthermore, the Src inhibitor PP2 does not prevent GPCR agonists from inhibiting Cx43-based gap junctional communication in either Rat-1 cells or primary astrocytes<sup>17</sup> (Table S1). Therefore, tyrosine phosphorylation of Cx43 leading to loss of cell-cell coupling, as observed with constitutively active c-Src and v-Src 24, may not actually occur under physiological conditions; an issue that warrants further investigation.

#### *Essential role for ZO-1*

Another novel finding of the present study concerns the role of ZO-1, an established binding partner of Cx43<sup>26,27</sup>. Originally identified as a major component of epithelial tight junctions<sup>59</sup>, ZO-1 is thought to serve as a platform to scaffold various transmembrane and cytoplasmic proteins. ZO-1 and its close relative ZO-2 have several protein-interaction domains, including three PDZ domains, one SH3 domain and one GUK domain. In epithelial cells, ZO-1 and ZO-2 act redundantly to some extent in the formation of tight junctions<sup>17,60</sup>. In non-epithelial cells lacking tight junctions, ZO-1 has been attributed a role in the assembly and stabilization of Cx43 gap junctions<sup>29,61</sup>, but its precise role has remained elusive. Our knock-down studies herein show that ZO-1 is essential for Gq/PLC-coupled receptors to inhibit intercellular communication, but not for coupling those receptors to PLC activation, as inferred from Ca<sup>2+</sup> mobilization experiments; this result suggests that loss of ZO-1 at Cx43 gap junctions is not compensated for by ZO-2. We find that ZO-1 binds directly to the very C-terminus of PLCβ3 via its third PDZ domain. In the simplest model compatible with our findings, ZO-1 serves to assemble Cx43 and PLCβ3 into a complex to permit regulation of gap junctional communication by localized changes in PtdIns(4,5)P<sub>2</sub>, as schematically illustrated in Fig. 8. Since we

found no evidence for direct binding of PtdIns(4,5)P<sub>2</sub> to Cx43 *in vitro*, PtdIns(4,5)P<sub>2</sub> might regulate junctional communication in an indirect manner, for example via a Cx43-associated protein that modifies the Cx43 regulatory tail and thereby shuts off channel function. Precisely how PtdIns(4,5)P<sub>2</sub> regulates the Cx43 multiprotein complex remains a challenge for future studies.

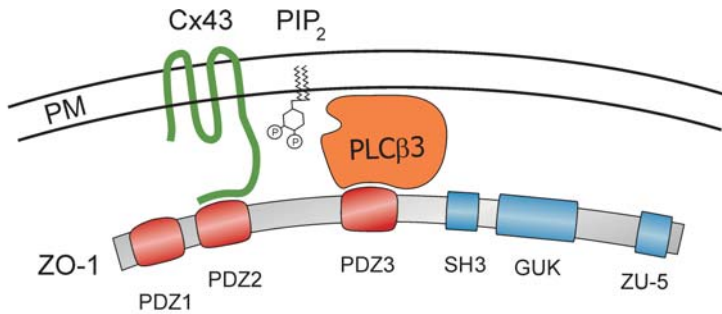


**Figure 8. Schematic drawing of the proposed model**

ZO-1 is proposed to assemble Cx43 and PLCβ3 into a complex, thereby facilitating regulation of Cx43 channel function by localized changes in PtdIns(4,5)P<sub>2</sub> upon receptor activation. Since we found no evidence for direct binding of PtdIns(4,5)P<sub>2</sub> to Cx43, PtdIns(4,5)P<sub>2</sub> might regulate junctional communication in an indirect manner, for example via a Cx43-associated protein that modifies the Cx43 regulatory tail and thereby shuts off channel function. PM, plasma membrane. See text for details.

## Materials and methods

### *Reagents*

Materials were obtained from the following sources: endothelin, thrombin receptor-activating peptide (TRP; sequence SFLLRN), neurokinin A, Cx43 polyclonal and  $\alpha$ -tubulin monoclonal antibodies from Sigma (St. Louis, MO); Pasteurella multocida toxin from Calbiochem-Novabiochem (La Jolla, CA); Cx43 NT monoclonal antibody from Fred Hutchinson Cancer Research Center (Seattle WA ); actin monoclonal from Chemicon International (Temecula, CA); polyclonal PLC $\beta$ 3 antibody from Cell Signalling; ZO-1 monoclonal antibody from Zymed; HRP-conjugated secondary antibodies from DAKO and secondary antibodies for immunofluorescence (goat-anti-mouse, Alexa488 and goat-anti-rabbit, Alexa594) from Molecular Probes. HA, Myc and GST monoclonal antibodies were purified from hybridoma cell lines 12CA5, 9E10 and 2F3, respectively. GFP antiserum was generated in our institute.

### *cDNA constructs*

Constructs encoding active (GTPase-deficient) G $\alpha$  subunits, eGFP-PHPLC $\delta$ 1, eCFP-PHPLC $\delta$ 1, eYFP-PHPLC $\delta$ 1, eGFP-tagged mouse type-I $\alpha$  PI(4)P 5-kinase have been described<sup>34,37,62</sup>. Mouse PLC $\beta$ 3 cDNA was obtained from MRC gene service, cloned into pcDNA3-HA by PCR (primers listed in Table S2) and ligated into pcDNA3-HA XhoI/NotI sites. HA-PLC $\beta$ 3- $\Delta$ PBD was obtained by restriction of the full-length construct with Eco47III, cleaving off the very C-terminal 14 residues. Human ZO-1 was cloned into XhoI and KpnI sites of pEGFP C2 (Clontech). GFP-based Yellow Cameleon 2.1 has been described<sup>34</sup>. Constructs encoding cytosolic 5-phosphatase fused to FKB12-mRFP and PM-FRB-CFP have been described<sup>43</sup>.

### *Cell culture and cell-cell communication assays*

Cells were cultured in DMEM containing 8% fetal calf serum, L-glutamine and antibiotics. For cell-cell communication assays, cells were grown in 3-cm dishes and serum starved for at least 4 hrs prior to experimentation. Monitoring the diffusion of Lucifer Yellow (LY) from single microinjected cells and single-electrode electrophysiological measurements of cell-cell coupling were done as described<sup>18</sup>. Images were acquired on a Zeiss Axiovert 135 inverted microscope, equipped with an Achroplan  $\times$  40 objective (N.A. 0.60) and a Nikon F301 camera.

### *SDS-PAGE, immunoblotting and immunoprecipitation*

Cells were harvested in Laemmli sample buffer (LSB), boiled for 10 min. and subjected to immunoblot analysis according to standard procedures. Filters were blocked in TBST/5% milk, incubated with primary and secondary antibodies, and visualized by enhanced chemoluminescence (Amersham Pharmacia). For immunoprecipitation, cells were harvested in 1% NP-40, 0.25% sodium desoxycholate lysis buffer. Lysates were spun down and the supernatants were subjected to immunoprecipitation using protein A-conjugated

antibodies for 4 hrs at 4°C. Proteins were eluted by boiling for 10 min. in LSB and analyzed by immunoblotting.

#### *Immunostaining and fluorescence microscopy*

Cells grown on coverslips were fixed in 3.7% formaldehyde in PBS for 15 min. Samples were blocked and permeabilized in PBS containing 1% BSA and 0.1% Triton X-100 for 30 min. Subsequently, samples were incubated with primary and secondary antibodies for 30 min. each in PBS/1% BSA, washed five times with PBS and mounted in MOWIOL (Calbiochem). Confocal fluorescence images were obtained on a Leica TCS NT (Leica Microsystems, Heidelberg, Germany) confocal system, equipped with an Ar/Kr laser. Images were taken using a 63x NA 1.32 oil objective. Standard filter combinations and Kalman averaging were used. Processing of images for presentation was done on a PC using the software package Photoshop (Adobe Systems Incorporated Mountain View, California, USA).

#### *Live-cell imaging*

All live imaging and time-lapse experiments were performed in bicarbonate-buffered saline containing (in mM) 140 NaCl, 5 KCl, 1 MgCl<sub>2</sub>, 1 CaCl<sub>2</sub>, 10 glucose, 23 NaHCO<sub>3</sub>, 10 HEPES (pH 7.2), kept under 5% CO<sub>2</sub> at 37°C. Images of live cells expressing GFP-PH and GFP-PIP5K were recorded on a Leica TCS-SP2 confocal microscope (Mannheim, Germany), using a 63x lens, N.A. 1.4.

#### *PtdIns(4,5)P<sub>2</sub>, IP<sub>3</sub> and Ca<sup>2+</sup> imaging by FRET ratiometry*

Temporal changes in PtdIns(4,5)P<sub>2</sub> levels in living cells were assayed by the FRET-based PtdIns(4,5)P<sub>2</sub> sensor, PH-PLCδ1, as described<sup>34</sup>. In brief, Rat-1 cells were transiently transfected with CFP-PH and YFP-PH constructs (1:1 ratio) using Fugene transfection agent and placed on a NIKON inverted microscope equipped with an Achromplan × 63 (oil) objective (N.A. 1.4). Excitation was at 425±5 nm. CFP and YFP emissions were detected simultaneously at 475±15 and 540±20 nm, respectively and recorded with PicoLog Data Acquisition Software (Pico Technology). FRET is expressed as the ratio of acceptor to donor fluorescence. At the onset of the experiment, the ratio was adjusted to 1.0, and FRET changes were expressed as relative deviations from base line. Temporal changes in IP<sub>3</sub> levels were monitored using a FRET-based IP<sub>3</sub> sensor, in which the IP<sub>3</sub>-binding domain of the human type-I IP<sub>3</sub> receptor (aa 224 to 605) is fused between CFP and YFP, essentially analogous to the sensor described previously<sup>63</sup>. In vitro binding studies showed that it bound IP<sub>3</sub> with an apparent K<sub>d</sub> of approx. 5 nM. Intracellular Ca<sup>2+</sup> mobilization was monitored using the CFP/YFP-based Ca<sup>2+</sup> sensor Yellow Cameleon 2.1<sup>32,34,64</sup>. Traces were smoothed in Microsoft Excel using a moving average function ranging from 3 to 6.

*PtdIns(4,5)P<sub>2</sub> depletion by rapamycin-induced translocation of phosphoinositide 5-phosphatase*

Rat-1 cells were transiently transfected with PM-CFP-FRB and mRFP-tagged FKBP-phosphoinositide 5-phosphatase (mRFP-FKBP-5-ptase)<sup>43</sup>. Cells were selected for experimentation when sufficient protein levels were expressed as judged by CFP and mRFP fluorescence. For PtdIns(4,5)P<sub>2</sub> measurements, the YFP-PH construct was cotransfected. For Ca<sup>2+</sup> measurements, cells were loaded with Oregon-Green-AM. To monitor gap junctional communication cells were loaded with calcein-AM and analyzed by Fluorescence Recovery After Photobleaching (FRAP)<sup>65</sup>. These experiments were performed on a Leica TCS-SP2 confocal microscope (Mannheim, Germany), using 63x lens, N.A. 1.4.

*Overexpression of PtdIns(4)P 5-kinase*

To overexpress PtdIns(4)P 5-kinase (PIP5K; type I $\alpha$ )<sup>62</sup>, virus containing the LZRS-PIP5K constructs was generated as described below. Rat-1 cells were incubated with 1 ml of viral supernatant supplemented with 10  $\mu$ l Dotap. 48 hrs after infection, cells were plated in selection medium. Transfected cells were selected on zeocin (200 $\mu$ g/ml, InVitrogen) for 2 weeks and colonies were examined for PIP5K expression.

*RNA interference*

To generate Cx43-deficient Rat-1 cells, Cx43 was knocked down by stable expression of retroviral pSuper (pRS)<sup>41</sup> containing the RNAi target sequence GGTGTGGCTGTCAGTGCTC. pRS-Cx43 was transfected into Phoenix-Eco package cells and the supernatant containing viral particles was harvested after 72 hrs. For infection, cells were incubated with 1 ml of viral supernatant supplemented with 10  $\mu$ l Dotap (Roche; 1 mg/ml). 48 hrs after infection, cells were selected on puromycin (2 $\mu$ g/ml) for 2 weeks. Single cell-derived colonies were tested for Cx43 expression and communication. PLC $\beta$ 3 was stably knocked down by retroviral expression of PLC $\beta$ 3 shRNA. Four different target sequences were selected, namely ACTACGTCTGCCTGCGAAATT, GATTTCGAGAGGTACTGGGC, TTACGTTGAGCCCGTCAAG, CCCTTTGACTTCCCCAAGG). Non-functional shRNA was used as a control. ZO-1 was transiently knocked down by adenoviral expression of ZO-1 RNAi. First, ZO-1 RNAi oligos containing the ZO-1 target sequence GGAGGGCCAGCTGAAGGAC were ligated into pSuper after oligo annealing. Next, the oligos together with the H1 RNA promotor were subcloned into pEntr1A (BamHI/XhoI) and recombined into pAd/PL-Dest according to protocol (Virapower Adenoviral Expression System; InVitrogen). Virus was produced in 293A packaging cells according to standard procedures. Supernatant containing virus particles was titrated on Rat-1 cells to determine the amount needed for ZO-1 knockdown.

## Acknowledgments

We thank Trudi Hengeveld and Ryanne Meems for assistance with the intercellular communication experiments and Jacco van Rheenen for imaging studies. T.B. and P.V. were supported in part by the Intramural Research Program of the National Institute of Child Health and Human Development of the National Institutes of Health. This work was supported by the Dutch Cancer Society and the Centre for Biomedical Genetics.

## Supplemental material

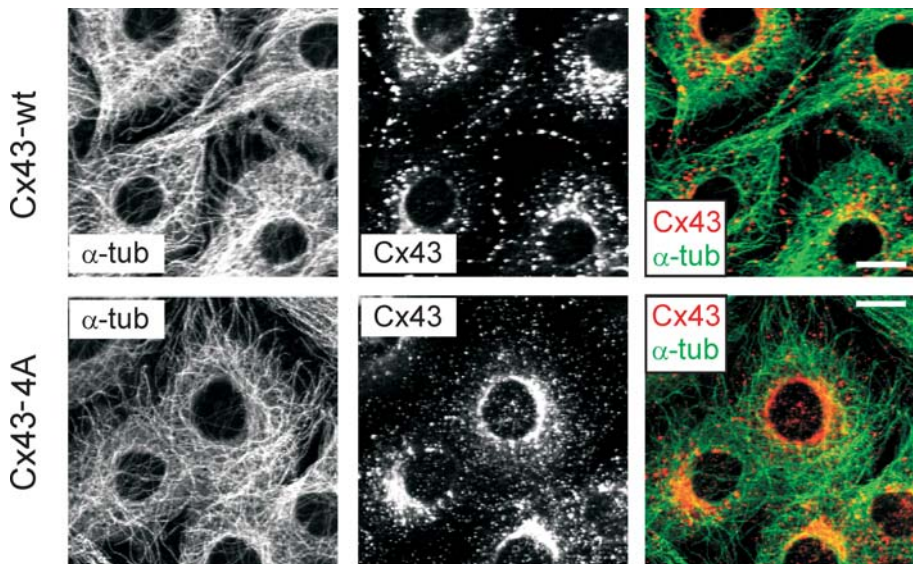


### Figure S1. Cx43-4A mutant accumulates intracellularly.

Confocal images of Cx43-deficient Rat-1 cells expressing wild-type Cx43(wt) and Cx43-4A, in which basic Arg/Lys residues in the C-terminal juxtamembrane domain were neutralized by mutation into Ala. Cells were immunostained for Cx43 (red) and  $\alpha$ -tubulin (green). Note intracellular accumulation of Cx43-4A and lack of detectable plasma membrane staining. Similar intracellular accumulation was observed with seven other Cx43(K/R->A) mutants, notably K237A,K241A; R239A,R243A; K241A,R243A; R239A,K241A; K237A,R239A; R239A,K241A,R243A; and K237A,R239A,K241A. Scale bars: 5  $\mu$ m.

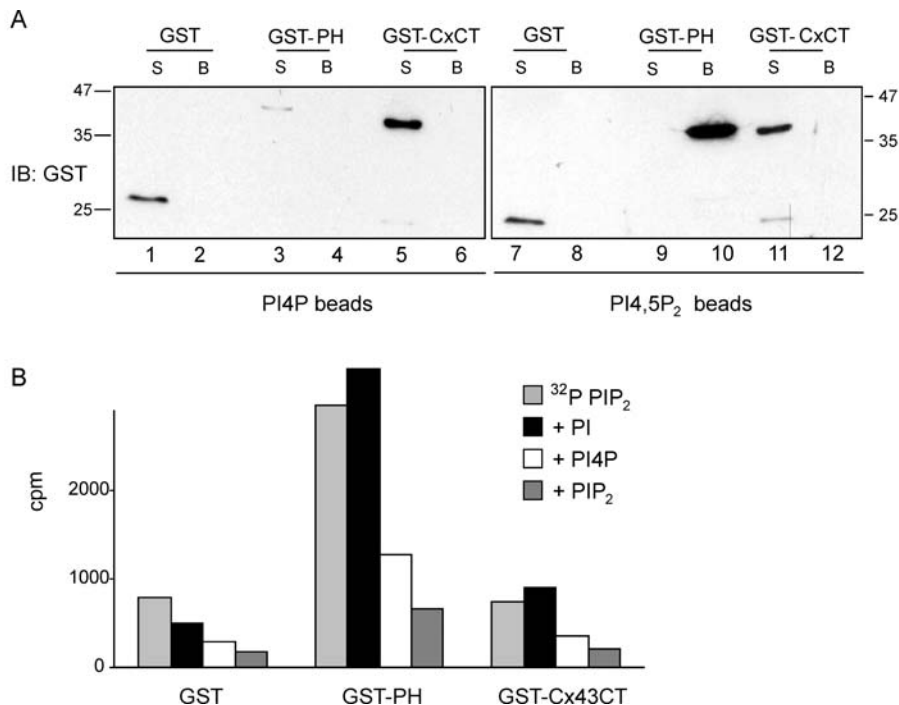


**Figure S2. No detectable phosphoinositide binding to the Cx43 C-terminal tail (CT).**

**A:** Pull-down of GST alone, GST-PH and GST-Cx43CT (aa 227-382) fusion proteins using PtdIns(4)P- and PtdIns(4,5)P<sub>2</sub>-coated agarose beads (Molecular Probes), as indicated. GST fusion proteins were purified from DH5 $\alpha$  bacteria following standard procedures. Anti-GST monoclonal antibody was purified from hybridoma cell line 2F3. 10 mg of GST or fusion protein was incubated with 7 ml of beads (~70 pmol) in 300 ml Triton-X100 buffer for 4 hrs at 4°C; beads were spun down by centrifugation. 20  $\mu$ l of the supernatant (S) was used as input control. Protein was eluted from the beads (B) by boiling for 10 min. in Laemmli sample buffer and analyzed by SDS-PAGE and immunoblotting for the presence of GST or GST-fusion protein.

**B:** Binding of  $^{32}\text{P}$ -labeled PtdIns(4,5)P<sub>2</sub> to GST fusion proteins. GST, GST-PH and GST-Cx43CT were coupled to glutathione beads and incubated with [ $^{32}\text{P}$ ]-PtdIns(4,5)P<sub>2</sub> alone or together with excess unlabeled PtdIns, PtdIns(4)P or PtdIns(4,5)P<sub>2</sub> for 1 hr at 4°C, as indicated. Beads were washed extensively (after centrifugation) and bound  $^{32}\text{P}$  activity was measured.

**Table S1. Pharmacological agents showing no effect on either basal or GPCR-regulated cell-cell communication.**

Cell-cell communication in Rat-1 cells was determined by LY diffusion. See also [18]

Agent	Concentration	Remarks
Phorbol ester: TPA (long-term) TPA (acute)	200 nM 100 nM	6- 24 hrs preincubation to downregulate PKC 0-15 min.
PC-PLC ( <i>B. cereus</i> )	1 U/ml	Generates diacylglycerol and activates PKC <sup>42</sup>
Pertussis toxin	200 ng/ml	6-16 hrs preincub.
Caged IP <sub>3</sub> Caged Ca <sup>2+</sup>		Transient rises in cytosolic Ca <sup>2+</sup> upon UV-induced uncaging
BAPTA-AM	5 mM	Ca <sup>2+</sup> signaling blunted
Nocodazole Cytochalasin D Rho-inactivating C3 toxin	10 μM 10 μM 100 ng/ml	Cell contraction <sup>58</sup>
Staurosporine  K252a PD598059 Ro-31-8220 PP2	100 μM  5 μM 10 μM 10 μM 50 μM	General protein kinase inhibitor (10 min. preincub.) General protein kinase inhibitor MAP kinase inhibitor PKC inhibitor Src family kinase inhibitor (20 min. preincub.)
Cycloheximide Brefeldin A  Monensin NH <sub>4</sub> Cl  Hyperosmotic sucrose	200 μM 5 μg/ml  5 μM 20 mM  0.5 M	60 min. preincub. 30 min. preincub.



**Table S2. Oligos used for cloning, mutagenesis and RNAi constructs.**

F, forward; R, reverse. All sequences 5'-&gt; 3'.

name	sequence
PLC $\beta$ 3 F	GATCCTCGAGTGGTAATCGATGGCGGGCGCGAGGCCCGGCG
PLC $\beta$ 3 R	GATCTCTAGAGCGGCCGCTCAAAGCTGGGTGTTTCTCTCTGGCTC
Cx43 RNAi F	GATCCCGGTGTGGCTGTCAAGAGAGAGCACTGACAGCCACAC- CTTTTGGAAA
Cx43 RNAi R	AGCTTTTCCAAAAAGGTGTGGCTGTCAAGAGAGCACT- GACAGCCACACCGGG
PLC $\beta$ 3 RNAi 1 F	GATCCCACTACGTCTGCCTGCGAAATTTCAAGAGAATTTGCGAGGCAGACG- TAGTGTTTTGGAAA
PLC $\beta$ 3 RNAi 1 R	AGCTTTTCCAAAAACTACGTCTGCCTGCGAAATTTCTTGAATTTGCGAG- GCAGACGTAGTGGGG
PLC $\beta$ 3 RNAi 2 F	GATCCCGATTTCGAGAGGTACTGGGCTTCAAGAGAGCCCAGTACCTCTC- GAATCTTTTGGAAA
PLC $\beta$ 3 RNAi 2 R	AGCTTTTCCAAAAAGATTTCGAGAGGTACTGGGCTCTTGAAGCCCAGTAC- CTCTCGAATCGGG
PLC $\beta$ 3 RNAi 3 F	GATCCCTTACGTTGAGCCCGTCAAGTTCAAGAGACTTGACGGGCTCAACG- TAATTTTGGAAA
PLC $\beta$ 3 RNAi 3 R	AGCTTTTCCAAAAATTACGTTGAGCCCGTCAAGTCTTGAAGTACGGGCT- CAACGTAAGGG
PLC $\beta$ 3 RNAi 4 F	GATCCCCCTTTGACTTCCCCAAGGTTCAAGAGACCTTGGGGAAGTCAAAG- GGTTTTTGGAAA
PLC $\beta$ 3 RNAi 4 R	AGCTTTTCCAAAAACCTTTGACTTCCCCAAGGTTCTTGAACCTT- GGGGAAGTCAAAGGGGGG
ZO-1 RNAi F	GATCCCGGAGGGCCAGCTGAAGGACTTCAAGAGAGTCCTTCAGCTGGCCCTC- CTTTTGGAAA
ZO-1 RNAi R	AGCTTTTCCAAAAAGGAGGGCCAGCTGAAGGACTCTTGAAGTCCT- TCAGCTGGCCCTCCGGG
Cx43 4A F	ACGGAGAAAACCATCTTCATCATCTTCATGCTGGTGGTGTCTTGGT- GTCTCTCGCTTTGAACATCATTGAGCTCTTCTACGTCTTCTCAAAGCGTT- GCGGATGCCGTGGCGGGAGCAAGCGATCCTTACCACGCCA
Cx43 4A R	GGCGTGGTAAGGATCGCTTGTCCCGCCACGGCATCCGCAACGCCTTTGAA- GAAGACGTAGAAGAGCTCAATGATGTTCAAAGCGAGAGACACCAAGGACAC- CACCAGCATGAAGATGATGAAGATGTTTCTC

**Reference list**

1. Goodenough, D. A., Goliger, J. A. & Paul, D. L. Connexins, Connexons, and Intercellular Communication. *Annual Review of Biochemistry* 65, 475-502 (1996).
2. Harris, A. L. Emerging issues of connexin channels: biophysics fills the gap. *Q Rev Biophys* 34, 325-472 (2001).
3. Saez, J. C., Berthoud, V. M., Branes, M. C., Martinez, A. D. & Beyer, E. C. Plasma membrane channels formed by connexins: their regulation and functions. *Physiol Rev* 83, 1359-1400 (2003).
4. Sohl, G. & Willecke, K. Gap junctions and the connexin protein family. *Cardiovascular Research* 62, 228-232 (2004).
5. Wei, C., Xu, X. & Lo, C. Connexins and cell signalling in development and disease. *Annual Review of Cell and Developmental Biology* 20, 811-838 (2004).
6. Reaume, A. G. et al. Cardiac malformation in neonatal mice lacking connexin43. *Science* 267, 1831-1834 (1995).
7. Mesnil, M., Crespin, S., Avanzo, J. & Zaidan-Dagli, M. Defective gap junctional intercellular communication in the carcinogenic process. *Biochimica et Biophysica Acta (BBA) - Biomembranes* 1719, 125-145 (2005).
8. Neijssen, J. et al. Cross-presentation by intercellular peptide transfer through gap junctions. *Nature* 434, 83-88 (2005).
9. Kwak, B. R., Pepper, M. S., Gros, D. B. & Meda, P. Inhibition of endothelial wound repair by dominant negative connexin inhibitors. *Mol Biol Cell* 12, 831-845 (2001).
10. Oliveira, R. et al. Contribution of gap junctional communication between tumour cells and astroglia to the invasion of the brain parenchyma by human glioblastomas. *BMC Cell Biol* 6, 7 (2005).
11. Qiu, C. et al. Targeting connexin43 expression accelerates the rate of wound repair. *Curr Biol* 13, 1697-1703 (2003).
12. Bernstein, S. A. & Morley, G. E. Gap junctions and propagation of the cardiac action potential. *Adv Cardiol* 42, 71-85 (2006).
13. Mori, R., Power, K. T., Wang, C. M., Martin, P. & Becker, D. L. Acute downregulation of connexin43 at wound sites leads to a reduced inflammatory response, enhanced keratinocyte proliferation and wound fibroblast migration. *J Cell Sci* 119, 5193-5203 (2006).
14. Gerido, D. A. & White, T. W. Connexin disorders of the ear, skin, and lens. *Biochim Biophys Acta* 1662, 159-170 (2004).
15. Venance, L., Piomelli, D., Glowinski, J. & Giaume, C. Inhibition by anandamide of gap junctions and intercellular calcium signalling in striatal astrocytes. *Nature* 376, 590-594 (1995).
16. Spinella, F. et al. Endothelin-1 Decreases Gap Junctional Intercellular Communication by Inducing Phosphorylation of Connexin 43 in Human Ovarian Carcinoma Cells. *J. Biol. Chem.* 278, 41294-41301 (2003).
17. Rouach, N. et al. S1P inhibits gap junctions in astrocytes: involvement of G and Rho GTPase/ROCK. *Eur J Neurosci* 23, 1453-1464 (2006).
18. Postma, F. et al. Acute loss of Cell-Cell Communication Caused by G Protein-coupled Receptors: A Critical Role for c-Src. *J. Cell Biol.* 140, 1199-1209 (1998).
19. Meme, W., Ezan, P., Venance, L., Glowinski, J. & Giaume, C. ATP-induced inhibition of gap junctional communication is enhanced by interleukin-1 beta treatment in cultured astrocytes. *Neuroscience* 126, 95-104 (2004).
20. Hill, C. S., Oh, S. Y., Schmidt, S. A., Clark, K. J. & Murray, A. W. Lysophosphatidic acid inhibits gap-junctional communication and stimulates phosphorylation of connexin-43 in WB cells:

- possible involvement of the mitogen-activated protein kinase cascade. *Biochem J* 303 ( Pt 2), 475-479 (1994).
21. Blomstrand, F. et al. Endothelins regulate astrocyte gap junctions in rat hippocampal slices. *Eur J Neurosci* 19, 1005-1015 (2004).
  22. Laird, D. Connexin phosphorylation as a regulatory event linked to gap junction internalization and degradation. *Biochimica et Biophysica Acta (BBA) - Biomembranes* 1711, 172-182 (2005).
  23. Lampe, P. & Lau, A. The effects of connexin phosphorylation on gap junctional communication. *The International Journal of Biochemistry & Cell Biology* 36, 1171-1186 (2004).
  24. Warn-Cramer, B. & Lau, A. Regulation of gap junctions by tyrosine protein kinases. *Biochimica et Biophysica Acta (BBA) - Biomembranes* 1662, 81-95 (2004).
  25. Giepmans, B. Gap junctions and connexin-interacting proteins. *Cardiovascular Research* 62, 233-245 (2004).
  26. Giepmans, B. & Moolenaar, W. The gap junction protein connexin43 interacts with the second PDZ domain of the zona occludens-1 protein. *Current Biology* 8, 931-934 (1998).
  27. Toyofuku, T. et al. Direct Association of the Gap Junction Protein Connexin-43 with ZO-1 in Cardiac Myocytes. *J. Biol. Chem.* 273, 12725-12731 (1998).
  28. Laing, J., Chou, B. & Steinberg, T. ZO-1 alters the plasma membrane localization and function of Cx43 in osteoblastic cells. *J Cell Sci* 118, 2167-2176 (2005).
  29. Hunter, A., Barker, R., Zhu, C. & Gourdie, R. Zonula Occludens-1 Alters Connexin43 Gap Junction Size and Organization by Influencing Channel Accretion. *Mol. Biol. Cell* 16, 5686-5698 (2005).
  30. Ponsioen, B., van Zeijl, L., Moolenaar, W. H. & Jalink, K. Direct measurement of cyclic AMP diffusion and signalling through connexin43 gap junctional channels. *Exp Cell Res* 313, 415-423 (2007).
  31. Orth, J., Lang, S., Taniguchi, M. & Aktories, K. Pasteurella multocida Toxin-induced Activation of RhoA Is Mediated via Two Families of G{alpha} Proteins, G{alpha}q and G{alpha}12/13. *J. Biol. Chem.* 280, 36701-36707 (2005).
  32. Rhee, S. Regulation of phosphoinositide-specific phospholipase C. *Annual Review of Biochemistry* 70, 281-312 (2001).
  33. Stauffer, T., Ahn, S. & Meyer, T. Receptor-induced transient reduction in plasma membrane PtdIns(4,5)P2 concentration monitored in living cells. *Current Biology* 8, 343-346 (1998).
  34. van der Wal, J., Habets, R., Varnai, P., Balla, T. & Jalink, K. Monitoring Agonist-induced Phospholipase C Activation in Live Cells by Fluorescence Resonance Energy Transfer. *J. Biol. Chem.* 276, 15337-15344 (2001).
  35. Varnai, P. & Balla, T. Visualization of Phosphoinositides That Bind Pleckstrin Homology Domains: Calcium- and Agonist-induced Dynamic Changes and Relationship to Myo-[3H] inositol-labeled Phosphoinositide Pools. *J. Cell Biol.* 143, 501-510 (1998).
  36. Halstead, J. R. et al. A role for PtdIns(4,5)P2 and PIP5Kalpha in regulating stress-induced apoptosis. *Curr Biol* 16, 1850-1856 (2006).
  37. Kranenburg, O. et al. Activation of RhoA by Lysophosphatidic Acid and Galpha 12/13 Subunits in Neuronal Cells: Induction of Neurite Retraction. *Mol. Biol. Cell* 10, 1851-1857 (1999).
  38. Cramer, H., Muller-Esterl, W. & Schroeder, C. Subtype-specific desensitization of human endothelin ETA and ETB receptors reflects differential receptor phosphorylation. *Biochemistry* 36, 13325-13332 (1997).
  39. Bremnes, T. et al. Regulation and intracellular trafficking pathways of the endothelin receptors. *J Biol Chem* 275, 17596-17604 (2000).

40. Alblas., van Etten I. & Moolenaar WH. Truncated, desensitization-defective neurokinin receptors mediate sustained MAP kinase activation, cell growth and transformation by a Ras-independent mechanism. *EMBO J* 15, 3351-3360 (1996).
41. Brummelkamp TR, B. R. A. R. A System for Stable Expression of Short Interfering RNAs in Mammalian Cells. *Science* 296, 550-553 (2002).
42. van Dijk, M. et al. Diacylglycerol generated by exogenous phospholipase C activates the mitogen-activated protein kinase pathway independent of Ras- and phorbol ester-sensitive protein kinase C: dependence on protein kinase C-zeta. *Biochem J* 323 ( Pt 3), 693-699 (1997).
43. Varnai, P., Thyagarajan, B., Rohacs, T. & Balla, T. Rapidly inducible changes in phosphatidylinositol 4,5-bisphosphate levels influence multiple regulatory functions of the lipid in intact living cells. *J Cell Biol* 175, 377-382 (2006).
44. Suh, B. C., Inoue, T., Meyer, T. & Hille, B. Rapid chemically induced changes of PtdIns(4,5)P<sub>2</sub> gate KCNQ ion channels. *Science* 314, 1454-1457 (2006).
45. Ponsioen, B., van Zeijl, L., Moolenaar, W. H. & Jalink, K. Direct measurement of cyclic AMP diffusion and signalling through connexin43 gap junctional channels. *Exp Cell Res* 313, 415-423 (2007).
46. Ponsioen, B., van Zeijl, L., Moolenaar, W. H. & Jalink, K. Direct measurement of cyclic AMP diffusion and signalling through connexin43 gap junctional channels. *Exp Cell Res* 313, 415-423 (2007).
47. Anderson, R., Boronenkov, I., Doughman, S., Kunz, J. & Loijens, J. Phosphatidylinositol Phosphate Kinases, a Multifaceted Family of Signalling Enzymes. *J. Biol. Chem.* 274, 9907-9910 (1999).
48. Hinchliffe KA., Ciruela A. & Irvine RF. PI(1-2)Pkins1, their substrates and their products: new functions for old enzymes. *Biochim Biophys Acta* 1436, 87-104 (1998).
49. Hilgemann, D. W., Feng, S. & Nasuhoglu, C. The complex and intriguing lives of PIP<sub>2</sub> with ion channels and transporters. *Sci STKE*. 2001, RE19 (2001).
50. Suh, B. C. & Hille, B. Regulation of ion channels by phosphatidylinositol 4,5-bisphosphate. *Curr Opin Neurobiol* 15, 370-378 (2005).
51. Hwang, J. et al. Regulation of Phospholipase C-beta 3 Activity by Na<sup>+</sup>/H<sup>+</sup> Exchanger Regulatory Factor 2. *J. Biol. Chem.* 275, 16632-16637 (2000).
52. Suh, P., Hwang, J., Ho Ryu, S., Donowitz, M. & Ho Kim, J. The Roles of PDZ-Containing Proteins in PLC-[beta]-Mediated Signalling. *Biochemical and Biophysical Research Communications* 288, 1-7 (2001).
53. Janmey, P. A., Lamb, J., Allen, P. G. & Matsudaira, P. T. Phosphoinositide-binding peptides derived from the sequences of gelsolin and villin. *J. Biol. Chem.* 267, 11818-11823 (1992).
54. McLaughlin, S. & Murray, D. Plasma membrane phosphoinositide organization by protein electrostatics. *Nature* 438, 605-611 (2005).
55. Giepmans, B. et al. Gap junction protein connexin-43 interacts directly with microtubules. *Current Biology* 11, 1364-1368 (2001).
56. Yin, H. L. & Janmey, P. A. Phosphoinositide regulation of the actin cytoskeleton. *Annu Rev Physiol* 65, 761-789 (2003).
57. Butkevich, E. et al. Drebrin Is a Novel Connexin-43 Binding Partner that Links Gap Junctions to the Submembrane Cytoskeleton. *Current Biology* 14, 650-658 (2004).
58. Giepmans, B., Hengeveld, T., Postma, F. & Moolenaar, W. Interaction of c-Src with gap junction protein connexin-43. Role in the regulation of cell-cell communication. *J. Biol. Chem.* 276, 8544-8549 (2001).

59. Stevenson, B. R., Siliciano, J. D., Mooseker, M. S. & Goodenough, D. A. Identification of ZO-1: a high molecular weight polypeptide associated with the tight junction (zonula occludens) in a variety of epithelia. *J. Cell Biol.* 103, 755-766 (1986).
60. Umeda, K. et al. Establishment and characterization of cultured epithelial cells lacking expression of ZO-1. *J Biol Chem* 279, 44785-44794 (2004).
61. Singh, D., Solan, J. L., Taffet, S. M., Javier, R. & Lampe, P. D. Connexin 43 interacts with zona occludens-1 and -2 proteins in a cell cycle stage-specific manner. *J Biol Chem* 280, 30416-30421 (2005).
62. van Horck, F., Lavazais, E., Eickholt, B., Moolenaar, W. & Divecha, N. Essential Role of Type I[alpha] Phosphatidylinositol 4-Phosphate 5-Kinase in Neurite Remodeling. *Current Biology* 12, 241-245 (2002).
63. Tanimura, A., Nezu, A., Morita, T., Turner, R. J. & Tojyo, Y. Fluorescent Biosensor for Quantitative Real-time Measurements of Inositol 1,4,5-Trisphosphate in Single Living Cells. *J. Biol. Chem.* 279, 38095-38098 (2004).
64. Miyawaki, A. et al. Fluorescent indicators for Ca<sup>2+</sup> based on green fluorescent proteins and calmodulin. *Nature* 388, 882-887 (1997).
65. Ponsioen, B., van Zeijl, L., Moolenaar, W. H. & Jalink, K. Direct measurement of cyclic AMP diffusion and signalling through connexin43 gap junctional channels. *Exp Cell Res* 313, 415-423 (2007).